

Capacitive sensor for tagless remote human identification using body frequency absorption signatures

*Original*

Capacitive sensor for tagless remote human identification using body frequency absorption signatures / Iqbal, Javed; Lazarescu, MIHAI TEODOR; BIN TARIQ, Osama; Arif, Arslan; Lavagno, Luciano. - In: IEEE TRANSACTIONS ON INSTRUMENTATION AND MEASUREMENT. - ISSN 0018-9456. - STAMPA. - 67:4(2018), pp. 789-797. [10.1109/TIM.2017.2789078]

*Availability:*

This version is available at: 11583/2687885 since: 2020-10-20T15:43:29Z

*Publisher:*

IEEE

*Published*

DOI:10.1109/TIM.2017.2789078

*Terms of use:*

This article is made available under terms and conditions as specified in the corresponding bibliographic description in the repository

*Publisher copyright*

IEEE postprint/Author's Accepted Manuscript

©2018 IEEE. Personal use of this material is permitted. Permission from IEEE must be obtained for all other uses, in any current or future media, including reprinting/republishing this material for advertising or promotional purposes, creating new collecting works, for resale or lists, or reuse of any copyrighted component of this work in other works.

(Article begins on next page)

# Capacitive sensor for tagless remote human identification using body frequency absorption signatures

Javed Iqbal, *IEEE IMS member*, Mihai Teodor Lazarescu, *IEEE member*, Osama Bin Tariq, *IEEE member*, Arslan Arif, *IEEE member* and Luciano Lavagno, *IEEE senior member*

**Abstract**—Although useful for many applications, the practical use of tagless remote human identification is often hampered by privacy, usability, reliability or cost concerns. In this article, we explore the use of capacitive sensors, which appear to address most of these concerns, to identify different persons based on the unique electric and dielectric properties of their bodies given by their specific tissue composition. We present experimental results obtained by measuring the capacitance of a  $16\text{ cm} \times 16\text{ cm}$  transducer plate 70 cm in front of different human bodies at different frequencies in the 5 kHz–160 kHz range. The measurements show clearly distinct signatures of capacitance variation with frequency for each person in the experiment, even after accounting for capacitance variations due to different body mass or physical dimensions. This work focuses on the contactless identification of human body using capacitive sensors in smart home environments.

**Index Terms**—capacitive sensing; tagless human sensing; tagless human identification; body frequency absorption signature; assisted living; smart home environments

## I. INTRODUCTION

Tagless remote human identification is significant for a wide range of applications, such as security, home and building automation, gaming and virtual reality, and assisted living. The latter is a growing issue as the world elderly population (aged 60 years or more) is rapidly increasing [1]. Estimates project the elderly population to 21.1% of the world population by 2050 [2]. Being at higher risk of health problems or falls [3], elderly people are a concern especially in highly industrialized societies [4].

Image- and video-based face and gait recognition are among the most widely used techniques for indoor human identification [5], [6]. C. Ding et al. presented a pose-invariant face recognition scheme for person identification [7]. A deep learning based face recognition technique is discussed in [8], while an unconstrained face detection and recognition approach is provided in [9]. A gait-based human identification method using arbitrary view transformation model was proposed by D. Muramatsu et al. [10]. Another biometric gait identification solution based on multilayer perception is presented in [11]. Thermal imaging-based face recognition systems can identify persons even in dark environments [12].

The methods proposed in [5]–[12] have good identification performance, but are expensive and hardly amenable for long-term battery-powered operation. Moreover, image-based techniques generally rise significant privacy concerns especially for smart home applications, healthcare monitoring and assisted living.

Pyroelectric infrared (PIR) sensors have been used for indoor human movement detection and identification, but with rather poor performance [13]. I. Al Naimi et al. presented a method for indoor human tracking and identification using capacitive floor tiles and PIR sensors, but it requires a costly smart floor to operate [14].

Wi-Fi signals have also been used for indoor person identification based on unique Wi-Fi spectrum perturbations that are caused by specific physiological features (e.g., height, weight) and behavioral traits (e.g., gait and repetitive movements of various body parts) [15], [16]. Y. Zeng et al. proposed a method to recognize the gait of a specific person among a small group of people based on monitoring the Channel State Information (CSI) of 802.11n devices [17].

Other indoor human identification techniques include Ultra-Wide Band (UWB) sensors [18], footstep-induced structural vibrations measured using geophone sensors [19], and ultrasonic sensors to detect body shape and movements [20].

Human identification techniques based on wearable Radio Frequency Identification (RFID) and Bluetooth tags [21], [22], [23] may often uncomfortably remind the persons that they are monitored, and the persons may forget to wear the tag which limits the reliability of the system.

Differences in human body physiological structure and composition can be detected also using capacitive sensors in order to identify the persons. The figure in [24, page 43] shows that the average human body permittivity ( $\epsilon$ ) and conductivity ( $\sigma$ ) vary with the frequency of the electric fields, and their values are much different than those of free space. The values vary also by tissue type [25], [26], [27], e.g., the average human body permittivity and conductivity are almost two-thirds those of the muscle tissue [24]. The electric properties of the human body also vary with age-related and gender-related changes in the body structure and composition [25], [28], [29].

In certain privacy-sensitive scenarios, we do not require too much details about the persons to be identified. For instance, in smart home applications a typical family may consist of elderly grandparents, a man, a woman and one

J. Iqbal, M.T. Lazarescu, O. Bin Tariq, A. Arif and L. Lavagno are with the Department of Electronics and Telecommunications, Politecnico di Torino, Corso Duca degli Abruzzi, I-10129, Torino, Italy (e-mail: {javed\_iqbal,mihai.lazarescu,osama.bintariq,luciano.lavagno}@polito.it).

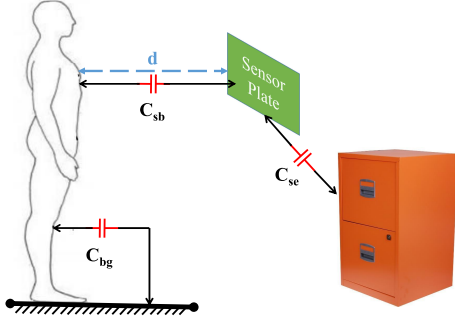


Fig. 1: Main components of the capacitance of a load mode capacitive sensor.

or more children, with different ages, weights, heights and possibly gender. They generally have significant differences in their body compositions due to factors like age, gender, weight, height, fat to muscle ratio, etc. In such applications, the differences in electric and dielectric properties of different human bodies can be exploited to successfully identify the members of a family of 4–6 people.

Capacitive sensors, especially those operating in load mode, are particularly interesting for long term indoor person and object monitoring and identification due to their relatively small size, low cost, low interface complexity, and low power requirements [30], [31], [32], [33], [34], [35]. Load-mode capacitive sensors operate using a single transducer plate which forms several capacitances with the environment and with the human body, such as those shown in Fig. 1:  $C_{sb}$  between the sensor and human body,  $C_{bg}$  between the human body and ground, and  $C_{se}$  between the sensor and the environment.

We propose in this work a method for human identification that is based mainly on  $C_{sb}$  dependency on the dielectric properties of the body [36]. In our previous work [35], we introduced a method for contactless indoor human identification using capacitive sensors, in which the capacitance of the human body measured at different frequencies was correlated with different body structures (see Fig. 2, reported here from previous work [35] with corrected amplitude gains and with the addition of the ideal one-pole low-pass gain for reference). In this work, we propose several improvements on the previous measurement method, which lead to significantly more resolution in the experimental results.

The rest of the article is organized as follows. Section II presents our main contributions, including a comparison with our previous work [35]. Section III explains the methodology of our experimentation. In Section IV, we present and discuss the experimental results. Section V concludes our work and highlights future developments.

## II. MAIN CONTRIBUTIONS

Building on the results of our previous work [35], we first propose several improvements of the measurement technique of the capacitance made between the sensor transducer and the human body, at different frequencies. Then we present the experimental results obtained using the new measurement

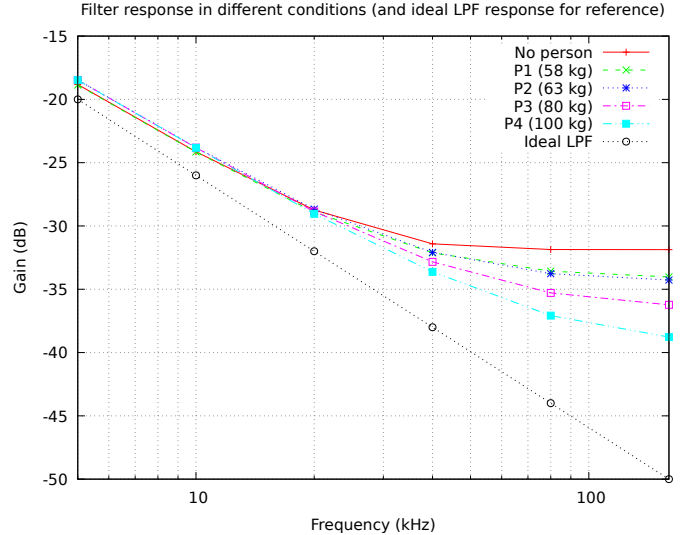


Fig. 2: Transducer gain dependency on measurement frequency for different body weights from our previous work [35], reported here with corrected amplitude gain values and the addition of the ideal low-pass filter response for reference.

method, which demonstrate significant gains in sensitivity and discrimination of the new method compared to the method used in our previous work.

Specifically, in our previous setting [35] we connected the capacitive transducer of the sensor as the capacitor in a first-order low-pass resistor-capacitor (RC) filter. We set the cutoff frequency of the filter one decade below the lowest measurement frequency, 5 kHz, and we measured the magnitude response of the filter for different human bodies over a wide excitation range, 5 kHz–160 kHz (shown in Fig. 2).

However, this measurement method has several limitations.

First, the gain measurements of the sensor lowpass RC filter were made at frequencies from 10 to 320 times higher than the filter cutoff frequency, thus in a frequency range that is strongly attenuated by the filter (by up to 50 dB). Moreover, the value of the resistor in the RC filter was very high (11 M $\Omega$ ) in order to set its cutoff frequency around 500 Hz, and this created a high impedance node that is highly susceptible to induced noise. The effect of the noise on the experimental results in [35] can be seen in Fig. 2, especially in the flattening of the sensor response at high frequencies. In fact, in that region the SNR can be very low, because on the one hand the signal is strongly attenuated (by up to 50 dB, close to the ideal LPF levels, and down to a few mV in amplitude), and on the other hand the noise level remains high due to the significant sensor susceptibility to noise. Since the RMS-to-DC detector of the sensor is equally sensitive to both signal and noise, at higher frequencies the RMS level is mostly given by the noise level, because the contribution of the signal is very reduced due to the low SNR. Consequently, the overall sensor sensitivity to capacitance variations due to specific body features is low, thus the sensor has a reduced sensitivity to human body composition and reduced discrimination capacity between different persons.

Secondly, because of the high contribution of the noise to the measurements at higher frequencies, variations of noise level due to the mere presence and physical form of a human body in its vicinity (e.g., because the body may partially shield the sensor from some noise sources) can be much larger than the usually small variations of an already low level signal (due to low SNR).

Thirdly, in our previous work we made a single set of measurements for each subject. For this reason, the previous results may have been affected by higher variability due to the high noise susceptibility and also several stochastic factors that can influence the overall capacitance of sensor transducer,  $C_S$ , such as variations in environmental relative humidity (RH), temperature (T) and other factors,

$$C_S = f(C_{sb}, C_{bg}, C_{se}, RH, T, \dots). \quad (1)$$

Compared to our previous work, the main contributions of this article are twofold.

First, we propose a significantly improved measurement method for the capacity of the sensor that addresses the limitations of the one used in our previous work [35]. The old method optimized the sensor sensitivity to transducer capacitance variations at the expense of the SNR. The improved method that we propose in this article avoids, at the same time, both the uneven attenuation of the various excitation frequencies, and also reduces the RC lowpass filter susceptibility to environmental noise. As we will show in the experimental results, with the new measurement method we were able to significantly increase the sensitivity of the sensor.

Secondly, we improve the measurement methodology to reduce the influence of the stochastic factors on the measurements by performing multiple measurements for each subject.

The experimental results that we present later in the article demonstrate the effectiveness of these improvements on both sensor sensitivity and its human body discrimination capability based on person-specific body composition.

### III. METHODOLOGY

As mentioned in Section I, the electric and dielectric properties of different tissues differ from person to person. C. Gabriel presented a comprehensive set of measurements of dielectric properties of different kinds of body tissues [36], which we summarize in TABLE I for the main body tissues for the frequencies of interest for our sensor. The measurements show marked differences between the properties of various tissue types, and since each person has a different body composition and physiology, we expect to obtain a body-specific variation pattern of the sensor capacitance when varying the measurement frequency.

Hence, with our method we measure the variations of the capacitance formed by a load-mode capacitive sensor with the body of different persons at various measurement frequencies. Then, we look at patterns of variation of the capacitance with the frequency which are person-specific.

#### A. Experimental procedure

The capacitance of interest for our measurements is formed between a capacitive sensor operating in load mode and a

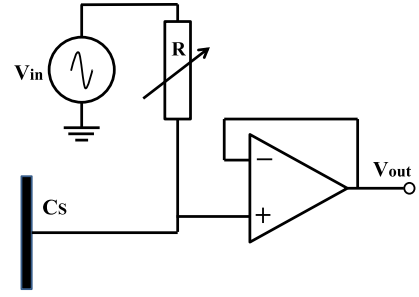


Fig. 3: Circuit used to tune the lowpass  $RC_S$  filter to the lowest excitation frequency used in our measurements, 5 kHz.

human body, when the distance between the sensor and the body, and other influencing factors are kept constant.

In this experiment, we measure the capacitance through its reactive effects at different frequencies. Specifically, we connect the capacitive sensor  $C_S$  in a first order lowpass RC filter configuration as shown in Fig. 3, we apply a sine wave on input,  $V_{in}$ , with known amplitude and frequency, and we obtain the output signal,  $V_{out}$ , by reading the filter output using a high impedance unity gain buffer. In this setting, the value of the sensor capacitance,  $C_S$ , determines the amplitude of the output signal,  $V_{out}$ .

Hence, for an input (excitation) signal

$$V_{in}(t) = A \sin(2\pi ft + \theta), \quad (2)$$

where

$$f = f_m = 5 \text{ kHz}, \quad (3)$$

with no person in sensor range we adjust the value of the lowpass filter resistor  $R$  to obtain an output voltage

$$V_{out}(t) = \frac{A}{\sqrt{2}} \sin\left(2\pi ft + \theta - \frac{\pi}{4}\right), \quad (4)$$

which is specific for a first order lowpass RC filter with the cutoff frequency equal to the excitation frequency,  $f_m$ . Then we measure the value of the resistor  $R$  and call it  $R_m$  (1.1 M $\Omega$  in our case), and use it as base value with which we build a resistor array as follows:  $R_m$ ,  $R_m/2$ ,  $R_m/4$ ,  $R_m/8$ ,  $R_m/16$  and  $R_m/32$ , as shown in Fig. 4.

There is no need to determine with high precision  $f_m$  or the resistor network, since the method is based on relative measurements and systematic errors typically cancel out. Much more important is the stability of the resistor values and of the excitation signal,  $V_{in}(t)$ , whose frequency we program as

$$f = 2^n f_m, \quad (5)$$

For each generated frequency (5), we select using an analog switch,  $S$ , the value of the resistor  $R$  that tunes the lowpass RC filter to the excitation frequency,

$$R = \frac{R_m}{2^n}, \quad (6)$$

where  $n = 0, 1, 2, 3, 4, 5$ .

By satisfying (2)–(6) at the same time, we make sure that the cutoff frequency of the lowpass RC filter is always tuned to the excitation frequency. This effectively eliminates the excessive

TABLE I: Variation of relative permittivity ( $\epsilon_r$ ) and electric conductivity ( $\sigma$ ) of major body tissues with the frequency.

Frequency (kHz)	Muscle		Fat		Bones		Breast fat	
	$\epsilon_r$	$\sigma$ (S/m)	$\epsilon_r$	$\sigma$ (S/m)	$\epsilon_r$	$\sigma$ (S/m)	$\epsilon_r$	$\sigma$ (S/m)
5	$6.0 \times 10^4$	$4.0 \times 10^{-1}$	$1.2 \times 10^3$	$1.8 \times 10^{-2}$	$1.4 \times 10^3$	$3.0 \times 10^{-3}$	$1.0 \times 10^3$	$11.0 \times 10^{-3}$
10	$3.0 \times 10^4$	$5.0 \times 10^{-1}$	$1.0 \times 10^3$	$1.8 \times 10^{-2}$	$1.2 \times 10^3$	$3.0 \times 10^{-3}$	$1.3 \times 10^2$	$11.0 \times 10^{-3}$
20	$1.0 \times 10^4$	$6.0 \times 10^{-1}$	$1.4 \times 10^2$	$1.8 \times 10^{-2}$	$1.1 \times 10^3$	$3.0 \times 10^{-3}$	$1.1 \times 10^2$	$11.0 \times 10^{-3}$
40	$1.4 \times 10^3$	$6.0 \times 10^{-1}$	$1.1 \times 10^2$	$1.9 \times 10^{-2}$	$1.05 \times 10^3$	$3.0 \times 10^{-3}$	$1.0 \times 10^2$	$11.0 \times 10^{-3}$
80	$1.1 \times 10^3$	$6.0 \times 10^{-1}$	$1.0 \times 10^2$	$1.9 \times 10^{-2}$	$1.0 \times 10^3$	$4.0 \times 10^{-3}$	$1.4 \times 10^1$	$11.0 \times 10^{-3}$
160	$2.9 \times 10^2$	$7.0 \times 10^{-1}$	$1.5 \times 10^1$	$1.9 \times 10^{-2}$	$1.9 \times 10^2$	$4.0 \times 10^{-3}$	$1.3 \times 10^{-1}$	$11.0 \times 10^{-3}$

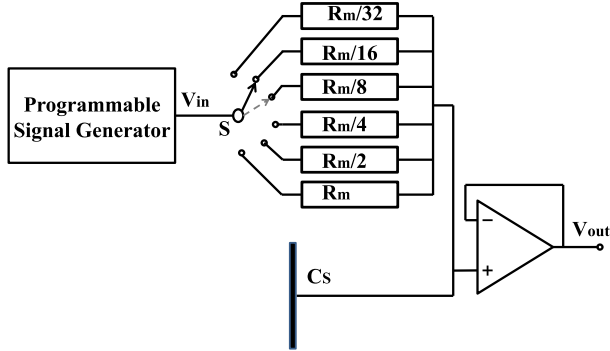


Fig. 4: Resistor network used to build first order lowpass filters tuned for each excitation frequency used in our measurements, from 5 kHz to 160 kHz.

attenuation of the higher frequencies from our previous method [35], significantly improving the sensor SNR. Importantly, in this case the differences in filter attenuation at various excitation frequencies can be mainly attributed to the differences in transducer capacitance induced by specific responses of the different body tissues at various excitation frequencies. We expect to obtain different attenuation patterns at various frequencies for different persons, which can ultimately be used to recognize the person in front of the sensor.

When the signal generator generates the excitation frequency given by (5), the analog switch  $S$  selects the resistor given by (6) to tune the  $RC_S$  lowpass filter cutoff frequency to the excitation frequency,

$$f_{c(n+1)} = 2^n f_m = \frac{1}{2\pi \frac{R_m}{2^n} C_S}. \quad (7)$$

Thus, we measure the output voltage,  $V_{out}$ , and calculate the gain of the lowpass  $RC_S$  filter as

$$\text{Gain} = 20 \log_{10} \left( \frac{V_{out}}{V_{in}} \right) \text{ (dB)}, \quad (8)$$

for each frequency determined by (7).

### B. Experimental setup

Fig. 5 shows the experimental setup. Based on our previous work [31], we have selected for these experiments a capacitive sensor made of a  $16 \text{ cm} \times 16 \text{ cm}$  metallic plate, installed at adult chest level. The plate is connected in a lowpass RC filter configuration as shown in Fig. 3.

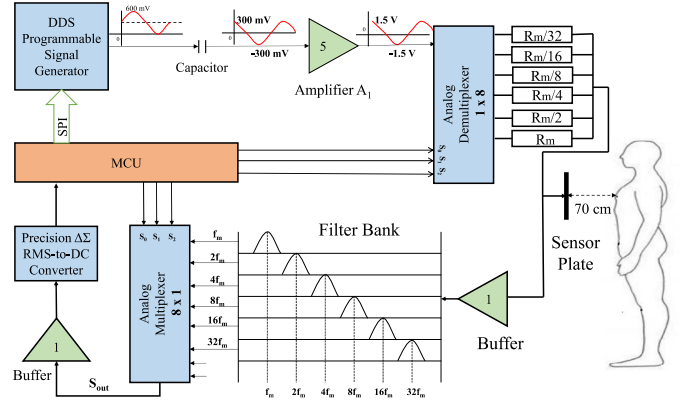


Fig. 5: Experimental setup. The microcontroller (MCU) programs the DDS to set, one at a time, the measurement excitation signals frequency in the 5 kHz–160 kHz range. To avoid markedly uneven attenuation for different excitation frequencies, the MCU selects then the resistor of the  $RC_S$  lowpass filter (made with the transducer capacitance), and the narrow bandpass filter for noise reduction, both tuned to the excitation frequency.

It is worth noting that the tissue composition of a human body changes with the height (generally, the human body composition at chest, abdomen, hips or legs level may be different). However, the differences in composition are less important for our proposed method, since we are interested only in relative measurements. In fact, we aim to distinguish the persons based on their specific frequency-capacitance signatures as they are recorded by the sensor from its height. The mounting height of the sensor should be chosen such way to include in its sensitivity zone the parts of the human body that are the most prone to have tissue composition variation between persons, but we leave this selection for future work.

The excitation frequency is generated using a direct digital synthesis (DDS) programmable signal generator, AD9837, programmed by an ATmega328P microcontroller using a serial peripheral interface (SPI) port. The DDS generates a  $600 \text{ mV}_{PP}$  sine wave with  $300 \text{ mV}$  DC offset, which we remove using a series capacitor.

The amplifier  $A_1$  brings the signal amplitude to  $3 \text{ V}_{PP}$ , which then enters the analog switch  $S$ . The switch is controlled by the microcontroller in sync with the DDS, in order to tune the cutoff frequency of the RC filter (made of the resistor selected by the switch and the capacitance of the plate) to match the

DDS-generated excitation frequency and satisfy (2)–(7).

The output of the lowpass  $\frac{R_m}{2^n} C_S$  filter is buffered and fed to a filter bank made of narrow band bandpass filters with a quality factor  $Q = 5$ . Each filter is centered on one of the possible excitation frequencies given by (7) and is used to reduce the signal noise. The filter is selected by the same microcontroller using an analog multiplexer, in sync with the programming of the DDS and with the position of the switch S.

The amplitude of the signal after the filter is converted to DC (demodulated) using a precision  $\Delta\Sigma$  RMS-to-DC converter and then measured using the microcontroller analog to digital converter (ADC).

This setup allows us to measure in sequence the capacitance of the sensor transducer at all frequencies given by (5), for a person standing at 70 cm in front of the sensor. Then we repeat the experiment for each person.

#### IV. EXPERIMENTAL RESULTS AND DISCUSSION

We used the sensor and the procedure described in Section III for four different persons with almost same height and age group, but with different physiological traits (weight, chest to waste ratio, Body Mass Index (BMI), hips to waste ratio, etc.), to ensure that the four selected persons are significantly different in their body compositions. In our focused application, i.e., smart home environments as mentioned in Section I, it is intuitive that the family members have comparatively much different body compositions. Hence, our sensor is expected to work relatively better in smart home applications.

As discussed in Section II, the capacitance  $C_S$  depends upon many variables, some of them stochastic, as shown in (1). Hence, we made ten measurements for each person.

##### A. Measurement results

The measurement results and their averages are shown in Fig. 6 for Persons 1, 2, 3 and 4 respectively. We note that they have a relatively low variance, which is due to stable experimental conditions and to the good SNR achieved using the improved capacitance measurement technique compared to our previous work [35].

The average attenuations of the lowpass filter for each person body are compared in Fig. 7. We note that the attenuations are shifted at all measurement frequencies by offsets correlated to the weight difference between the person bodies. We consider that this correlation has two main components:

- 1) the direct correlation between the physical body dimensions and the transducer capacitance;
- 2) the direct correlation between the physical dimensions of the body and its weight.

For the former, we can see from Fig. 1 that the physical dimensions of the person body directly influence the  $C_{sb}$  component of the total transducer capacitance (more specifically, larger body dimensions increase  $C_{sb}$ ). For the latter, human bodies with different weights usually have different physical dimensions, and heavier bodies are usually associated with larger dimensions. Hence, we obtain that heavier bodies tend

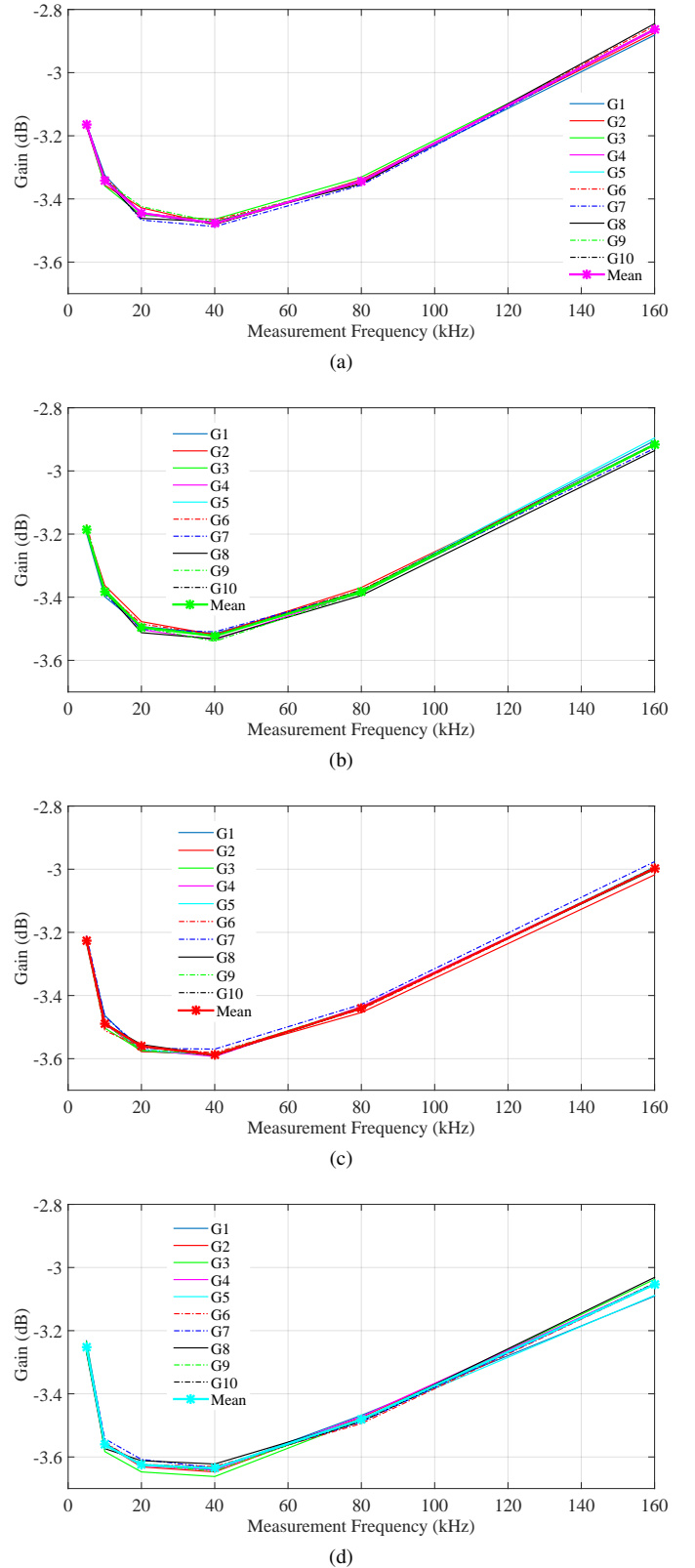


Fig. 6: Ten measurements (and their average) of the  $RC_S$  filter gain at different frequencies for: Person 1 (a), Person 2 (b), Person 3 (c), and Person 4 (d).

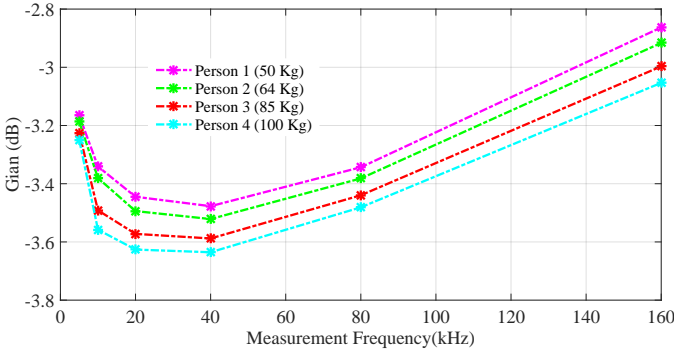


Fig. 7: Average  $RC_S$  filter gains at different frequencies for the four persons. We note that a higher body weight is typically associated with larger body size, which generally increases the capacitance of the transducer, hence the attenuation of the lowpass filter used for capacitance measurement.

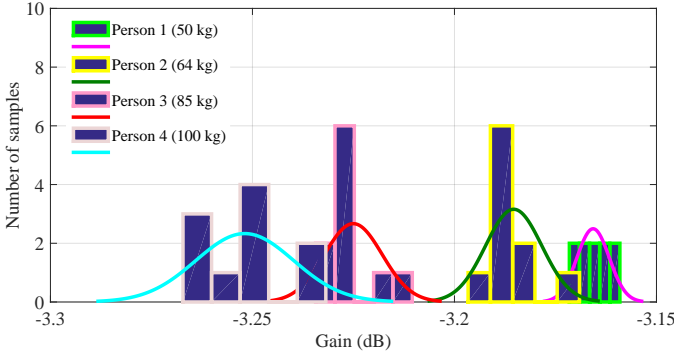


Fig. 8: Measurements distributions at  $f_c = 5$  kHz.

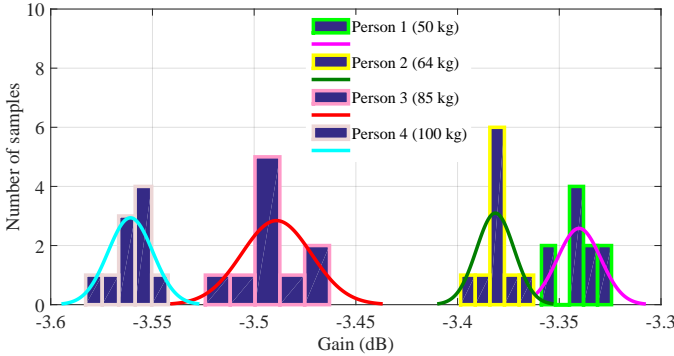


Fig. 9: Measurements distributions at  $f_c = 10$  kHz.

to increase  $C_{sb}$ , which increases the attenuation of the lowpass filter (see Fig. 4).

Fig. 8, 9, 10, 11, 12 and 13 show the distributions of the measured  $RC_S$  lowpass filter gains for each body at the filter cutoff frequencies of 5 kHz, 10 kHz, 20 kHz, 40 kHz, 80 kHz and 160 kHz respectively. As explained for Fig. 7, we note also here that the separations between the gain distributions for each body are correlated with the difference in body weights.

For practical uses, an adequate trade-off should be found between the length of the measurement and the speed of movement of the subject in front of the sensor, to optimize the measurement accuracy. Averaging a higher number of

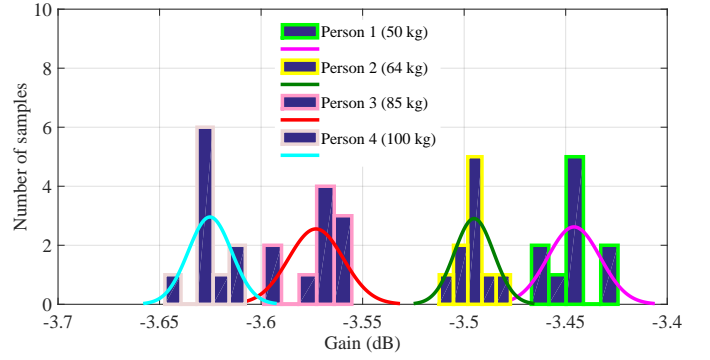


Fig. 10: Measurements distributions at  $f_c = 20$  kHz.

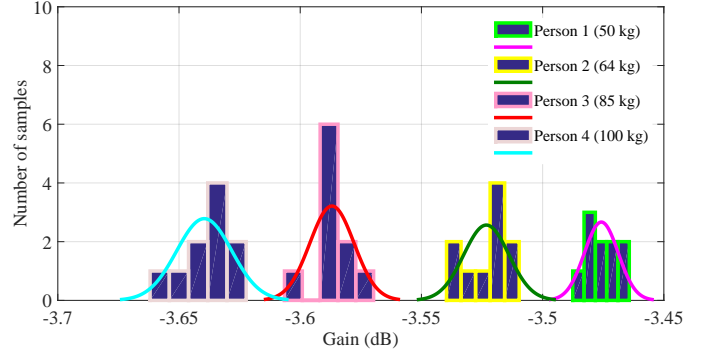


Fig. 11: Measurements distributions at  $f_c = 40$  kHz.

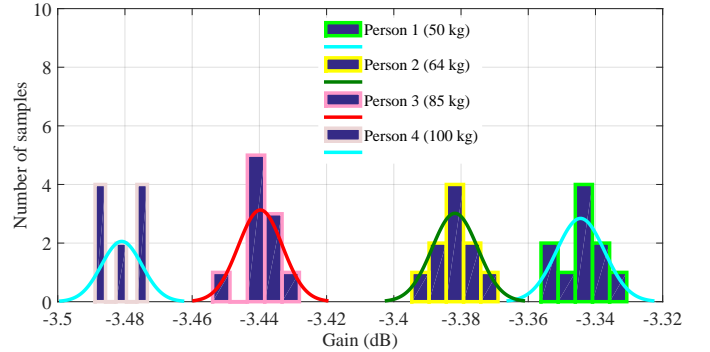


Fig. 12: Measurements distributions at  $f_c = 80$  kHz.

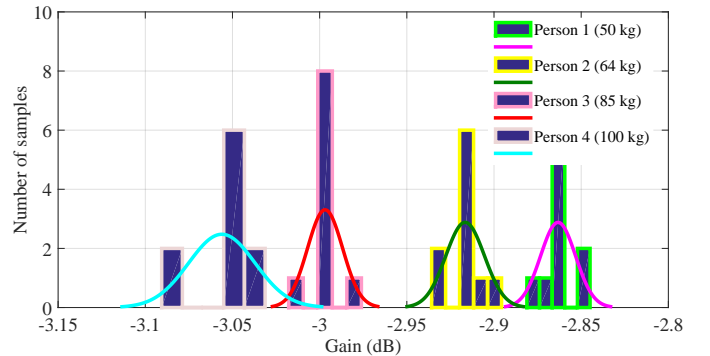


Fig. 13: Measurements distributions at  $f_c = 160$  kHz.

measurements can reduce noise and increase accuracy, while a significant change in position of the subject during the mea-

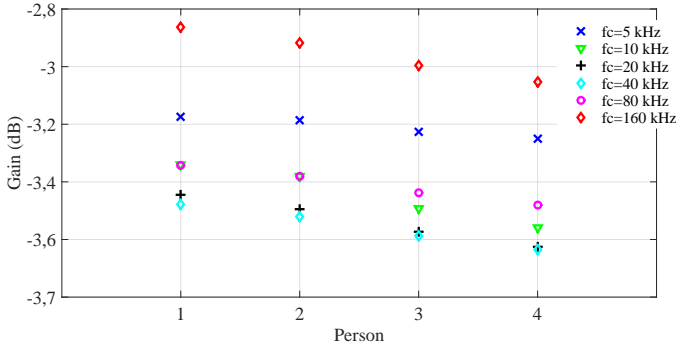


Fig. 14:  $RC_S$  lowpass filter gain for each person at different frequencies shows a distinct pattern for each person.

measurements can reduce the accuracy. For instance, our sensor needs 50 ms to acquire one reading, hence ten successive readings averaged to reduce noise influence will require about 500 ms. This measurement time can be adequate for practical applications where the subject does not move significantly within 500 ms, but since the variance of the readings is reduced (see Fig. 6, 8, 9, 10, 11, 12, 13), the average over a lower number of successive readings can be used for applications in which the subject is expected to move faster.

### B. Person identification

Using these experimental data, we expect to be able to identify the person in front of the sensor from a pool of known persons by examining the relative capacitance values measured at different frequencies for each person.

For this purpose, in Fig. 14 we show for each person the variation of the transducer capacitance with the measurement frequency.

First, we note that the measurements have different levels for each person. The level shifts can be mostly attributed to the differences in body dimensions, which are mostly due to different person weights.

Secondly, we notice a different attenuation pattern for each person, when the measurement frequency varies. We attribute the difference in patterns to differences in tissue composition for each person, which can determine different electric and dielectric properties for each body according to measurements in TABLE I.

In Fig. 15 we show how the frequency-dependent attenuation patterns can be processed for automatic identification of the person using machine learning classification algorithms. First, each set of attenuations is independently normalized in order to remove most of its dependencies on body weight. Then, the classification algorithm uses only the remaining (inner) normalized values (measured at frequencies between 10 kHz and 80 kHz) for the typical machine learning phases of training, validation and classification. It should be noted that the absolute values of the outer frequencies of our measurement range, 5 kHz and 160 kHz, contribute through the normalization to the pattern of the inner frequencies normalized values, which is the one used for person identification.

Hence, we consider that the relative variation pattern of body capacitance with the frequency can constitute a reliable

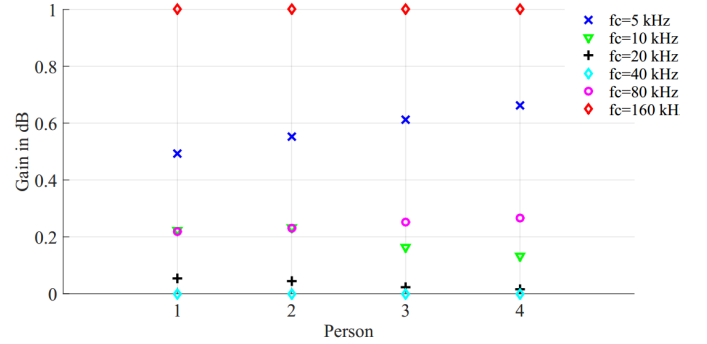


Fig. 15: Normalized  $RC_S$  lowpass filter gains at different frequencies show a distinct pattern for each person that depends on the unique composition of each person body, and which can be used for person identification.

means to identify the person, because the patterns depend mostly on person-specific body composition.

Nevertheless, there can be practical cases where the resolution of the system is not sufficient to distinguish closely matching persons. In such cases, we expect poor recognition results.

## V. CONCLUSIONS AND FUTURE WORK

In this article we presented a method for tagless remote identification of humans that is based on body absorption signatures detected using a capacitive sensor that operates at different frequencies. The technique leverages the different electric and dielectric properties of the main tissues in the human body, and the fact that each body has a unique composition.

This method extends and significantly enhances our previous work [35], improving considerably the sensitivity and discrimination capability of the sensor.

The experimental results, acquired at 70 cm distance using a 16 cm  $\times$  16 cm metallic plate as a capacitive sensor in load mode, show that four male individuals with different body compositions produce distinct capacitance variation patterns to frequencies between 5 kHz and 160 kHz. The patterns remain well distinct after normalizing them to exclude the capacitive effects of the different dimensions and mass of the bodies.

The system uses single-plate sensors and can be produced to be easily installed in the door frames of an indoor space, where it can monitor the persons passing through the doors.

In future work we intend to explore the variations of sensor sensitivity with variability factors such as relative humidity, temperature, clothing, transpiration, distance to human body, body orientation, measurement frequency ranges, and if the method can be reliably used for gender identification.

The response time of our sensor to acquire one set of measurements over all the excitation frequencies is almost 50 ms. We intend to explore the ways to speed up the measurement in order to make the method applicable in real life (dynamic) contexts, to fuse information from multiple sensors to improve the accuracy in such contexts, to perform automatic person

identification using machine learning classification, and to reduce the power consumption for long-term service using either battery or wireless power.

#### ACKNOWLEDGMENT

The authors would like to thank Guo Qinglang, Abubakar Siddique Muqaddas, Malik Ashter Mehdy and Zohaib Aziz who were the subject of our experimentation and who provided us with their precious time during the execution of our experimentation.

#### CONFLICTS OF INTEREST

The authors declare no conflict of interest.

#### REFERENCES

- [1] S. Blackman, C. Matlo, C. Bobrovitskiy, A. Waldoch, M. L. Fang, P. Jackson, A. Mihailidis, L. Nygård, A. Astell, and A. Sixsmith, "Ambient assisted living technologies for aging well: a scoping review," *Journal of Intelligent Systems*, vol. 25, no. 1, pp. 55–69, 2016.
- [2] F. Erden, S. Velipasalar, A. Z. Alkar, and A. E. Cetin, "Sensors in Assisted Living: A survey of signal and image processing methods," *IEEE Signal Processing Magazine*, vol. 33, no. 2, pp. 36–44, 2016.
- [3] F. Buckinx, Y. Rolland, J.-Y. Reginster, C. Ricour, J. Petermans, and O. Bruyère, "Burden of frailty in the elderly population: perspectives for a public health challenge," *Archives of Public Health*, vol. 73, no. 1, p. 19, 2015.
- [4] M. S. North and S. T. Fiske, "Modern attitudes toward older adults in the aging world: A cross-cultural meta-analysis," *Psychological bulletin*, vol. 141, no. 5, p. 993, 2015.
- [5] C. Ding and D. Tao, "A comprehensive survey on pose-invariant face recognition," *ACM Transactions on intelligent systems and technology (TIST)*, vol. 7, no. 3, p. 37, 2016.
- [6] T. K. Lee, M. Belkhatir, and S. Sanei, "A comprehensive review of past and present vision-based techniques for gait recognition," *Multimedia tools and applications*, vol. 72, no. 3, pp. 2833–2869, 2014.
- [7] C. Ding, C. Xu, and D. Tao, "Multi-task pose-invariant face recognition," *IEEE Transactions on Image Processing*, vol. 24, no. 3, pp. 980–993, 2015.
- [8] E. Zhou, Z. Cao, and Q. Yin, "Naive-deep face recognition: Touching the limit of LFW benchmark or not?" *arXiv preprint arXiv:1501.04690*, 2015.
- [9] B. F. Klare, B. Klein, E. Taborsky, A. Blanton, J. Cheney, K. Allen, P. Grother, A. Mah, and A. K. Jain, "Pushing the frontiers of unconstrained face detection and recognition: IARPA Janus Benchmark A," in *Proceedings of the IEEE Conference on Computer Vision and Pattern Recognition*, 2015, pp. 1931–1939.
- [10] D. Muramatsu, A. Shiraishi, Y. Makihara, M. Z. Uddin, and Y. Yagi, "Gait-based person recognition using arbitrary view transformation model," *IEEE Transactions on Image Processing*, vol. 24, no. 1, pp. 140–154, 2015.
- [11] V. B. Semwal, M. Raj, and G. C. Nandi, "Biometric gait identification based on a multilayer perceptron," *Robotics and Autonomous Systems*, vol. 65, pp. 65–75, 2015.
- [12] R. S. Ghiass, O. Arandjelovic, H. Bendada, and X. Maldague, "Infrared face recognition: a literature review," in *The 2013 International Joint Conference on Neural Networks (IJCNN)*. IEEE, 2013, pp. 1–10.
- [13] J. Yun and S.-S. Lee, "Human movement detection and identification using pyroelectric infrared sensors," *Sensors*, vol. 14, no. 5, pp. 8057–8081, 2014.
- [14] I. Al-Naimi, C. B. Wong, P. Moore, and X. Chen, "Advanced approach for indoor identification and tracking using smart floor and pyroelectric infrared sensors," in *Information and Communication Systems (ICICS), 2014 5th International Conference on*. IEEE, 2014, pp. 1–6.
- [15] T. Xin, B. Guo, Z. Wang, M. Li, Z. Yu, and X. Zhou, "FreeSense: Indoor Human Identification with Wi-Fi Signals," in *Global Communications Conference (GLOBECOM), 2016 IEEE*. IEEE, 2016, pp. 1–7.
- [16] J. Zhang, B. Wei, W. Hu, and S. S. Kanhere, "Wifi-id: Human identification using wifi signal," in *Distributed Computing in Sensor Systems (DCOSS), 2016 International Conference on*. IEEE, 2016, pp. 75–82.
- [17] Y. Zeng, P. H. Pathak, and P. Mohapatra, "WiWho: wifi-based person identification in smart spaces," in *Proceedings of the 15th International Conference on Information Processing in Sensor Networks*. IEEE Press, 2016, p. 4.
- [18] G. Mokhtari, Q. Zhang, C. Hargrave, and J. C. Ralston, "Non-Wearable UWB Sensor for Human Identification in Smart Home," *IEEE Sensors Journal*, vol. 17, no. 11, pp. 3332–3340, 2017.
- [19] S. Pan, N. Wang, Y. Qian, I. Velibeyoglu, H. Y. Noh, and P. Zhang, "Indoor person identification through footstep induced structural vibration," in *Proceedings of the 16th International Workshop on Mobile Computing Systems and Applications*. ACM, 2015, pp. 81–86.
- [20] N. Khalil, D. Benhaddou, O. Gnawali, and J. Subhlok, "Nonintrusive Occupant Identification by Sensing Body Shape and Movement," in *BuildSys@ SenSys*, 2016, pp. 1–10.
- [21] M. Shahzad and A. X. Liu, "Probabilistic optimal tree hopping for RFID identification," *IEEE/ACM Transactions on Networking*, vol. 23, no. 3, pp. 796–809, 2015.
- [22] S. Nainan, R. Parekh, and T. Shah, "RFID technology based attendance management system," *arXiv preprint arXiv:1306.5381*, 2013.
- [23] R. Lodha, S. Gupta, H. Jain, and H. Narula, "Bluetooth smart based attendance management system," *Procedia Computer Science*, vol. 45, pp. 524–527, 2015.
- [24] B. J. Klauenberg and D. Miklavcic, *Radio frequency radiation dosimetry and its relationship to the biological effects of electromagnetic fields*. Springer Science & Business Media, 2012, vol. 82.
- [25] C. Gabriel, S. Gabriel, and E. Corthout, "The dielectric properties of biological tissues: I. Literature survey," *Physics in medicine and biology*, vol. 41, no. 11, p. 2231, 1996.
- [26] S. Gabriel, R. Lau, and C. Gabriel, "The dielectric properties of biological tissues: II. Measurements in the frequency range 10 Hz to 20 GHz," *Physics in medicine and biology*, vol. 41, no. 11, p. 2251, 1996.
- [27] —, "The dielectric properties of biological tissues: III. Parametric models for the dielectric spectrum of tissues," *Physics in medicine and biology*, vol. 41, no. 11, p. 2271, 1996.
- [28] A. Peyman, C. Gabriel, E. Grant, G. Vermeeren, and L. Martens, "Variation of the dielectric properties of tissues with age: the effect on the values of SAR in children when exposed to walkie-talkie devices," *Physics in medicine and biology*, vol. 54, no. 2, p. 227, 2008.
- [29] A. Peyman, "Dielectric properties of tissues; variation with age and their relevance in exposure of children to electromagnetic fields; state of knowledge," *Progress in biophysics and molecular biology*, vol. 107, no. 3, pp. 434–438, 2011.
- [30] A. Braun, R. Wichert, A. Kuijper, and D. W. Fellner, "Capacitive proximity sensing in smart environments," *Journal of Ambient Intelligence and Smart Environments*, vol. 7, no. 4, pp. 483–510, 2015.
- [31] A. Ramezani Akhmareh, M. T. Lazarescu, O. Bin Tariq, and L. Lavagno, "A Tagless Indoor Localization System Based on Capacitive Sensing Technology," *Sensors*, vol. 16, no. 9, p. 1448, 2016.
- [32] I. Al-Naimi and C. B. Wong, "Indoor human detection and tracking using advanced smart floor," in *Information and Communication Systems (ICICS), 2017 8th International Conference on*. IEEE, 2017, pp. 34–39.
- [33] A. Arshad, S. Khan, A. Z. Alam, R. Tasnim, T. S. Gunawan, R. Ahmad, and C. Nataraj, "An activity monitoring system for senior citizens living independently using capacitive sensing technique," in *Instrumentation and Measurement Technology Conference Proceedings (I2MTC), 2016 IEEE International*. IEEE, 2016, pp. 1–6.
- [34] J. Iqbal, M. T. Lazarescu, O. B. Tariq, and L. Lavagno, "Long range, high sensitivity, low noise capacitive sensor for tagless indoor human localization," in *7th IEEE International Workshop on Advances in Sensors and Interfaces (IWASI), 2017, Vieste, Italy*. IEEE, 2017, pp. 189–194.
- [35] J. Iqbal, A. Arif, O. B. Tariq, M. T. Lazarescu, and L. Lavagno, "A contactless sensor for human body identification using RF absorption signatures," in *IEEE Sensors Applications Symposium (SAS2017), New Jersey, USA*, 2017, pp. 1–6.
- [36] C. Gabriel, "Compilation of the Dielectric Properties of Body Tissues at RF and Microwave Frequencies." King's College London (United Kingdom) Dept. of Physics, Tech. Rep., 1996.

## AUTHORS BIOGRAPHIES



**Javed Iqbal** received his Masters of Science in Telecommunications Engineering from Politecnico di Torino, Italy in 2014. Currently he is a Ph.D. student at Department of Electronics and Telecommunications (DET), Politecnico di Torino, Italy. His areas of interest are Instrumentation and Measurements, Statistical signal Processing and Control Systems. He is currently working on the design and implementation of low power sensors for indoor human detection, localization, tracking and identification.



**Mihai Teodor Lazarescu** received his Ph.D. from Politecnico di Torino (Italy) in 1998. He was Senior Engineer at Cadence Design Systems, founded several startups and serves now as Assistant Professor at Politecnico di Torino. He co-authored more than 40 scientific publications and several books. His research interests include sensors for indoor localization, reusable WSN platforms, high-level hardware/software co-design and high-level synthesis of WSN applications.



**Osama Bin Tariq** received the MS degree in Electronic engineering with specialization in embedded systems from the Politecnico di Torino, Italy where currently he is pursuing the Ph.D. degree with the department of Electronic and Telecommunications engineering. His research interests include sensing systems for health monitoring, indoor localization and machine learning.



**Arslan Arif** received his Masters of Science from National University of Sciences and Technology, Pakistan. Currently he is a Ph.D. student at the Department of Electronics and Telecommunications (DET), Politecnico di Torino, Italy. His research interests include High level synthesis, computation accelerators and Internet of things (IoT).



**Luciano Lavagno** received the Ph.D. degree in EECS from the University of California at Berkeley, Berkeley, CA, USA, in 1992. He was the architect of the POLIS HW/SW co-design tool. From 2003 to 2014, he was an Architect of the Cadence CtoSilicon high-level synthesis tool. Since 1993, he has been a Professor with the Politecnico di Torino, Italy. He co-authored four books and more than 200 scientific papers. His research interests include synthesis of asynchronous circuits, HW/SW co-design, high-level synthesis, and design tools for wireless sensor networks.

networks.